



pubs.acs.org/JACS Article

Yeast Mitochondria Import Aqueous Fe^{II} and, When Activated for Iron—Sulfur Cluster Assembly, Export or Release Low-Molecular-Mass Iron and Also Export Iron That Incorporates into Cytosolic Proteins

Rachel E. Shepherd, Alexia C. Kreinbrink, Cybele Lemuh Njimoh, Shaik Waseem Vali, and Paul A. Lindahl*



Cite This: J. Am. Chem. Soc. 2023, 145, 13556–13569



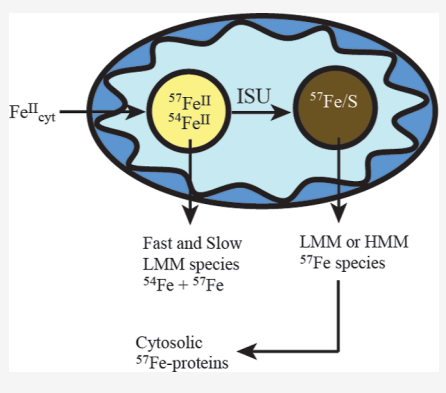
ACCESS I

III Metrics & More

Article Recommendations

Supporting Information

ABSTRACT: Iron—sulfur cluster (ISC) assembly occurs in both mitochondria and cytosol. Mitochondria are thought to export a low-molecular-mass (LMM) iron and/or sulfur species which is used as a substrate for cytosolic ISC assembly. This species, called X—S or (Fe—S)_{int}, has not been directly detected. Here, an assay was developed in which mitochondria were isolated from ⁵⁷Fe-enriched cells and incubated in various buffers. Thereafter, mitochondria were separated from the supernatant, and both fractions were investigated by ICP-MS-detected size exclusion liquid chromatography. Aqueous ⁵⁴Fe^{II} in the buffer declined upon exposure to intact ⁵⁷Fe-enriched mitochondria. Some ⁵⁴Fe was probably surface-absorbed but some was incorporated into mitochondrial iron-containing proteins when mitochondria were activated for ISC biosynthesis. When activated, mitochondria exported/released two LMM nonproteinaceous iron complexes. One species, which comigrated with an Fe-ATP complex, developed faster than the other Fe species, which also comigrated with phosphorus.



Both were enriched in ⁵⁴Fe and ⁵⁷Fe, suggesting that the added ⁵⁴Fe entered a pre-existing pool of ⁵⁷Fe, which was also the source of the exported species. When ⁵⁴Fe-loaded ⁵⁷Fe-enriched mitochondria were mixed with isolated cytosol and activated, multiple cytosolic proteins became enriched with Fe. No incorporation was observed when ⁵⁴Fe was added directly to the cytosol in the absence of mitochondria. This suggests that a different Fe source in mitochondria, the one enriched mainly with ⁵⁷Fe, was used to export a species that was ultimately incorporated into cytosolic proteins. Iron from buffer was imported into mitochondria fastest, followed by mitochondrial ISC assembly, LMM iron export, and cytosolic ISC assembly.

INTRODUCTION

Iron—sulfur clusters (ISCs) are found in many metalloproteins that engage in a wide variety of cellular functions. In eukaryotes, these clusters are biosynthesized in both mitochondria and cytosol. Curiously, mitochondrial ISC assembly is independent of the cytosolic assembly process, whereas cytosolic ISC assembly depends on the mitochondria. The molecular-level mechanism giving rise to this asymmetry has been investigated for over 2 decades but is only partially understood.

In Saccharomyces cerevisiae, mitochondrial ISC assembly begins with the import of cytosolic Fe^{II} ions through Mrs3/4, high-affinity transporters on the inner membrane. The nomenclature for *S. cerevisiae* proteins is used.) Once imported, these ions comprise a low-molecular-mass (LMM) pool of iron in the mitochondrial matrix. Iron from this pool is likely used as a substrate for ISC (and heme) biosynthesis. Cysteine desulfurase (Nfs1) extracts sulfur from cysteine in a large protein complex that serves as the site of [Fe₂S₂] biosynthesis. Iron then binds Isu1/2, scaffold proteins for ISC biosynthesis.

The cysteine-derived sulfurs on Nfs1 becomes the bridging sulfide ions in ISCs. Assembled $[Fe_2S_2]$ clusters are transferred to Grx5, a monothiol glutaredoxin in mitochondria. Some Grx5-bound clusters are transferred to a complex composed of Isa1/Isa2/Iba57 proteins which assembles $[Fe_4S_4]$ clusters. 10,11 Once assembled, $[Fe_4S_4]$ and $[Fe_2S_2]$ clusters are installed into at least 19 mitochondrial apo-proteins. 12

ISC assembly in the cytosol involves the Cytosolic Iron–sulfur Assembly system a.k.a. the CIA. This system assembles $[Fe_4S_4]$ clusters and installs them into approximately 19 cytosolic and 10 nuclear apo-proteins. The source of Fe and S used in this process is uncertain. The best-supported hypothesis regarding the sulfur substrate, proposed by Lill and

Received: December 16, 2022 Published: June 20, 2023





co-workers nearly 25 years ago, is that a LMM species named X–S is synthesized by the mitochondrial ISC assembly machinery and exported into the cytosol for use by the CIA.¹ The source of iron was not specified; it might be associated with X–S, or it might originate from cytosolic Fe^{II}, perhaps associated with the labile iron pool (Figure 1).

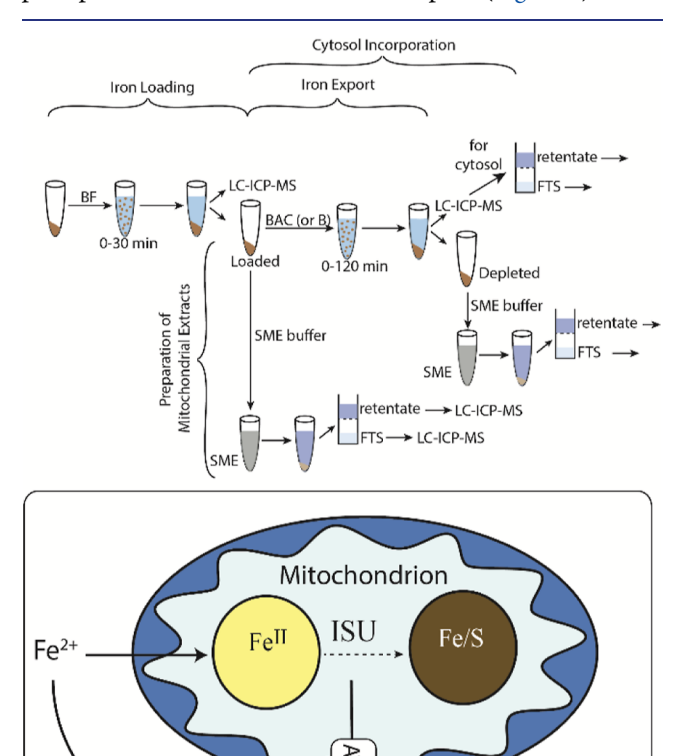


Figure 1. Overview of the procedures used (top) and the commonly assumed iron trafficking pathway in yeast involving X-S and or (Fe-S)_{int} (bottom). Top: For iron loading, freshly isolated mitochondria were resuspended in BF buffer for various time points and then centrifuged into the supernatant and pellet fractions. Supernatants were analyzed by LC-ICP-MS. Pellets were converted into SMEs which were separated by filtering into retentate and FTS fractions. In other experiments, loaded mitochondria were incubated in various buffers, separated into the supernatant and pellet, and then analyzed similarly. In a third type of experiment, the mitochondria were incubated in buffers containing isolated cytosol. Supernatants from experiments involving cytosol buffers were separated into retentate and FTS fractions. Bottom: cytosolic iron is thought to enter the mitochondria, be processed by the ISC assembly machinery, and then be exported as X-S/(Fe-S)_{int} through Atm1 for incorporation into cytosolic ISC proteins via the CIA. A less likely scenario is that cytosolic iron is used directly for cytosolic ISC assembly without mitochondrial involvement.

"X-S"

or Fe-Sint

Cytosol

Cytosolic

Clusters

Iron Sulfur

CIA

X–S is thought to be exported through Atm1, an inner membrane ABC half-transporter that couples the hydrolysis of ATP to the transport of a LMM species across the membrane. Glutathione (GSH) and the IMS protein Erv1 are also involved. Atm1 is a homodimer with two transmembrane domains and two ATP binding domains facing the matrix. The presence of a binding site that

accommodates GSH suggests that Atm1 binds and transports GSH or a related sulfur species such as the oxidized form of glutathione, disulfide GSSG.²⁰ Balk and co-workers used Atm1-incorporated membrane vesicles to show that Atm1 exports GSSG and trisulfide (GS-S⁰-SG) but not GSH.²¹ Lill has argued that there is no need for cells to export GSSG from the mitochondria since they contain a mitochondrial glutathione reductase which could reduce any GSSG that formed. Moreover, GSSG is likely synthesized in the cytosol.¹⁵ Balk suggested that X—S may be GS-S⁰-SG, with the bridging sulfane serving as the substrate for the CIA.

Using an in vitro ³⁵S-radioactive assay, Pain and co-workers have demonstrated that intact isolated mitochondria, when treated with an activation cocktail composed of cysteine, NADH, NADPH, ATP, and GTP, export a LMM sulfur-containing species called S_{int} that is used in cytosolic tRNA thiolation. ^{22–24} Whether S_{int} is identical to X–S is uncertain. S_{int} passes through a 3 kDa cut-off filter, suggesting a low-mass species, and chromatograms of chloroform-extracted S_{int}-containing solutions exhibit S-based peaks with apparent masses between 700 and 1100 Da. Biosynthesis of S_{int} requires functional Nfs1 and Isu1/2 (but not Ssq1) and export requires Atm1. Pandey et al. (2018) concluded that S_{int} serves as a substrate for thiolation reactions that incorporate sulfur into cytosolic tRNA molecules. ^{3,22,25}

Cowan and co-workers have proposed that X–S is a $[Fe_2S_2]$ cluster coordinated by four glutathione ligands and have synthesized a hydrolytically stable $\{[Fe_2S_2](GS)_4\}^{2-}$ cluster. Moreover, Atm1-empregnated proteoliposomes reportedly transport this cluster across a membrane in an ATP-dependent fashion, and the ATPase activity of Atm1 is stimulated by $\{[Fe_2S_2](GS)_4\}^{2-}$. A recent cryo-electron microscopy structure of an Atm1 homologue has unresolved "cargo" bound, with dimensions consistent with an $[Fe_2S_2](GS)_4$ cluster. Lill has expressed doubts that a $\{[Fe_2S_2](GS)_4\}^{2-}$ cluster can be sufficiently stabilized in aqueous aerobic environments and has cautioned about interpreting the stimulation of ATPase activity by the synthetic cluster because GSH, which alone stimulates the activity, might have dissociated from the cluster. List

Nevertheless, Cowan's proposal is attractive because it also explains how X–S might communicate the status of mitochondrial ISC assembly activity to gene–expression activities in the nucleus. Transcription factors Aft1 and Aft2 control the expression of ~20 genes known as the iron regulon. When these proteins bind $[Fe_2S_2]$ clusters, they migrate out of the nucleus and into the cytosol, deactivating the iron regulon. According to this scenario, the WT levels of exported X–S suppress (through Aft1/2 migration) the activation of these genes, whereas low levels activate them. This explains why Atm1-deficient cells, unable to export X–S, are iron-dysregulated. 30

Pandey et al. presented evidence that Atm1 also exports an iron- and sulfur-containing LMM species which they named (Fe-S)_{int}.³¹ Using an ³⁵S-based assay that includes Fe^{II} ascorbate in the activation cocktail, they found that mitochondrial Fe and S are installed into cytosol-bound apoferredoxin (Yah1). By utilizing the mutations of specific proteins involved in mitochondrial ISC biosynthesis, they found that all such proteins are required for (Fe-S)_{int} export. In contrast, S_{int} export requires that the ISC assembly pathway operates only to the step at which Nfs1 acts. Both species are

exported at higher levels in the presence of an acceptor protein or tRNA.

In Pandey's assay, isolated mitochondria are incubated in solutions containing (a) isolated cytosol (or buffer); (b) [$^{35}\mathrm{S}$]-cysteine; (c) activation nucleotides ATP, GTP, and NADH; (d) Fe 11 ascorbate; and (e) a truncated form of Yah1 (apo- $\Delta N60$) which accepts assembled [Fe $_2\mathrm{S}_2$] ISCs in the cytosol. After incubating for 30 min at 30 °C, the suspension is spun by centrifugation, separating mitochondria from the supernatant. The supernatants are subjected to native PAGE, and bands enriched in $^{35}\mathrm{S}$ are detected by autoradiography. Using WT mitochondria, $^{35}\mathrm{S}$ is incorporated into tRNAs, apo- $\Delta N60$ Yah1, and apo-aconitase, a mitochondrial [Fe $_4\mathrm{S}_4$] protein. $^{35}\mathrm{S}$ is not incorporated into these targets when mitochondria are excluded in the assay.

Here, we modified the Pandey assay and used an anaerobic refrigerated liquid chromatography system with an on-line ICP-MS to detect two LMM iron species that were exported or released from the mitochondria. We also detected import of a LMM iron complex into the mitochondria, installation of iron from the imported complex into mitochondrial proteins, and installation of mitochondrial iron into cytosolic proteins.

EXPERIMENTAL SECTION

Metal Stock Solutions. Solutions were prepared using highpurity water (HPW) from a Teflon sub-boiling still (Savillex). The 54 Fe metal powder was dissolved in concentrated trace-metal-grade (TMG) nitric acid (see Table S1 for the source of all reagents). In earlier preparations, 54 Fe II ascorbate was generated by adding sodium ascorbate to the acidic iron stock until pH = 5. In later preparations, a 20-fold molar excess of the ascorbate relative to iron was added. The resulting 54 Fe II ascorbate solutions were stored in a glovebox (MBraun Labmaster 130) at ~4 °C and <10 ppm O2 as monitored by a Teledyne model 3110 meter. 57 Fe citrate was prepared by dissolving 57 Fe2O3 in concentrated TMG HCl, diluting with HPW, treating with sufficient sodium citrate to attain pH = 5, and then filtering through a 0.2 μm filter (Millipore). The 100 mM CuSO4 stock was prepared in water and sterilized by passage using a 0.2 μm filter.

Growth of Cells. *S. cerevisiae* W303 cells were grown under respiring conditions in complete synthetic media (Sunrise Science) supplemented with 3% glycerol and 1.7 g/L YNB prior to autoclaving. To cooled autoclaved media was added 1% ethanol, 1 μ M CuSO₄, and 10 μ M 57 Fe^{III} citrate from stock solutions (all final concentrations).

Mitochondria Isolation. All steps after harvesting cells were performed in a refrigerated anaerobic glovebox. All buffers were degassed on a Schlenk line prior to import into the box. The cells (typically 70 g wet) were resuspended in ABC buffer (100 mM ammonium bicarbonate pH 7.5 and 1 mM EDTA) and 10 mM DTT for 10 min at 30 °C. (Buffer names are indicated in bold when defined and are compiled in Table S2.) The resuspended cells were treated with zymolyase (2.5 mg/g of wet cells) that had been dissolved in ABCSN buffer (20 mM ABC buffer pH 7.5, 1.2 M sorbitol, 60 mM NaCl, and 1 mM EDTA). The samples were incubated for 1-1.5 h until the OD600 of a 1:100 dilution of the sample in buffer was reduced to <20% of the original OD600 and centrifuged at 5000g to pellet spheroplasts. The resulting spheroplasts were washed in ABCSN buffer and then resuspended in ~200 mL of ABCSE buffer (20 mM ABC pH 7.4, 0.6 M sorbitol, and 1 mM EDTA) with 1 mM PMSF. The spheroplast suspensions were homogenized in 40 mL fractions for 25 strokes with a Dounce homogenizer (ACE glass) and a "B" pestle. The resulting lysate was spun by centrifugation at 2000g for 5 min (Sorvall Lynx 6000). The supernatant was collected, and the pellet was resuspended in ABCSE buffer. The resuspended pellet was rehomogenized for 10 additional strokes. The resulting lysate was spun by centrifugation at 2000g for 5 min. The second supernatant

was collected and combined with the first supernatant, and the resulting solution was centrifuged at 4000g for 5 min. The supernatant was collected and recentrifuged under the same conditions. The supernatant was collected and recentrifuged at 12,000g for 10 min. The pellet containing crude mitochondria was resuspended in ~10 mL of ABCS buffer (20 mM ABC pH 7.4 + 0.6 M sorbitol but no EDTA or PMSF). An aliquot of the resuspension was diluted 1:50 with HPW, and the protein concentration was determined (typically 10-15 mg/mL) using the BCA assay (Pierce). The remaining suspension (10 mg per gradient) was carefully overlaid on six 32-60% (w/v) sucrose in 20 mM ABC pH 7.5 buffer gradients (10 mL in each layer) and centrifuged for 1 h at 150,000g with no break applied (Beckman Optima L-90k Ultracentrifuge, 32.1Ti rotor, 32,000 rpm). For a typical preparation, 3 rounds of centrifugations (18 gradients total) were required. The brown bands at the 32-60% sucrose interfaces were collected, combined, and diluted 3× with B buffer (20 mM ammonium acetate pH 6.5 plus 0.6 M sorbitol). The resulting suspension was centrifuged at 12,000g for 10 min. The pellet was typically resuspended in 10 mL of B buffer. The resulting suspension was defined to be isolated mitochondria. The concentration of protein in the suspension was determined as described above. The typical yields ranged from 100 to 170 mg mitochondrial protein.

Western Blots. The purity of isolated mitochondria was determined via western blot. ³² In brief, an SDS-PAGE of isolated mitochondria and whole cell lysate was run (Nupage 10% Bis-Tris acrylamide gel), and the gel was transferred to a PVDF membrane. The membranes were incubated for 1 h in a milk-**TBST** (Trisbuffered saline with 0.1% Tween 20) solution while rocking prior to adding primary antibodies. The membranes were incubated overnight while rocking at 4 °C and then washed 5× for 5 min each in TBST. The membranes were incubated in secondary antibody-HRP for 1 h at RT. After being washed 5× for 5 min in TBST, the membranes were incubated in the enhanced chemiluminescence (Pierce) solution for 1 min before being imaged (Fujifilm LAS 4000 mini).

Iron Import into Mitochondria. In this and the other two assays described below, mitochondria were used without freezing within 30 min of isolation. The resuspended mitochondria were divided into 15 mg aliquots in 2 mL plastic epi-tubes and centrifuged at 12,000g for 10 min (Southwest Science microcentrifuge). Assays were initiated (t=0) by resuspending the mitochondrial pellets in 1.5 mL of either buffer B or buffer BF (the same as B but with either 2 or 10 μ M ⁵⁴Fe^{II} ascorbate, from the stock) that had been chilled to -5 °C (Boekel MicroCooler II). Some suspensions were centrifuged (as above) immediately after mixing (t=0); others were incubated for t=10 or 20 min and then centrifuged. Supernatants were passed through a 0.2 μ m filter (Titan3 17 mm filter RC membrane, Thermo Scientific) and typically injected onto the LC column (see below).

Soluble Mitochondrial Extracts. Pellets from the experiment just described were washed (resuspended with 1.5 mL of buffer B, centrifuged, and supernatant decanted) and then resuspended in 500 μ L of **SME** buffer (20 mM AA pH 6.5 + 2% triton). Suspensions were vortexed briefly and then centrifuged at 14,000g for 15 min. The supernatant, designated soluble mitochondrial extract (SME), was passed through a 10 kDa filter (Amicon Ultra 0.5 mL ultracel 10k). The resulting flow-through solution (FTS) (100 μ L) was injected onto a Superdex Peptide or 30 Increase column (Cytiva) equilibrated in 20 mM ammonium acetate pH 6.5 mobile phase flowing at 0.6 mL/min. The corresponding retentate was diluted to 500 μ L using HPW, then passed through a 0.2 μ m filter, and injected onto either a Superdex 200 or a Superdex 200 Increase column (Cytiva).

Export or Release of LMM Mitochondrial Iron into Buffer. The isolated mitochondria suspended in buffer B were typically divided into 7–12 aliquots (15 mg protein each) and centrifuged as described above. Each pellet was resuspended in 1.5 mL of BF buffer (10 mg/mL, final concentration of mitochondrial proteins) at 30 °C (Fisher Mini Dry Bath) and incubated for 15 min. The resulting 54 Feloaded mitochondria were centrifuged for 10 min at 12,000g. Supernatants were passed through a 0.2 μ m filter prior to LC injections. The corresponding pellets were washed with buffer B, resuspended in either buffer B or BAC (t = 0), and incubated at either

-5 or 30 °C. Buffers were brought to room temperature prior to incubation. After various incubation times (t = 0...120 min), the suspensions were centrifuged for 10 min at 12,000g. The resulting supernatants were filtered for LC-ICP-MS analysis, and SMEs were prepared as described above for eventual analysis.

Export of Mitochondrial Iron into the Cytosol. Cytosol was isolated as described³³ using buffer B. Aliquots (15-20 mL) of the resulting Bcyt buffer (isolated cytosol in B buffer) were frozen for later use. BACcyt buffer was prepared similarly but also adding (as powders) all AC components present in BAC buffer to aliquots of Bcyt buffer, achieving the same final concentrations as in BAC buffer. The assay was performed as described above but using buffer Bcyt or BACcyt rather than B or BAC. If Bcyt and BACcyt buffers contained <0.75 mg/mL protein, they were concentrated using a 3 kDa centrifugal filter as needed to achieve that concentration.

An assay was initiated (t=0) by resuspending a 54 Fe-loaded mitochondrial pellet in either Bcyt or BACcyt buffer. Assay solutions were incubated for t = 0-120 min at 30 °C and then centrifuged for 10 min at 12,000g. SMEs were prepared from the resulting pellets, and supernatants were passed through a 10 kDa centrifuge filter, concentrating the retentate fractions $\sim 3 \times$. Retentates ($\sim 500 \mu L$) were passed through a 0.2 μ m filter and then injected onto the Superdex 200 or 200 Increase column using 20 mM ammonium acetate pH 6.5 mobile phase buffer flowing at 0.6 mL/min. The LC-ICP-MS system has been described.³⁴ Some samples were injected onto a "ghost column" consisting of PEEK (polyetheretherketone) tubing in place of the column. Standard solutions of ATP, NADH, GTP, ADP, GSH, GSSG, and cysteine were prepared as described.³

Various proteins (thyroglobulin, alcohol dehydrogenase, albumin, amylase, carbonic anhydrase, and cytochrome c) and low mass molecules (cyanocobalamin and GSH) were used as standards for a calibration curve. Standards were injected onto the Superdex 200 column and detected at 280 nm. Thyroglobulin was used to determine the void volume as it was above the resolving capacity of the column. A calibration curve was constructed (log molecular weight of standards vs ratio of elution/void volumes) to estimate apparent molecular masses.

Iron Concentration Determinations. The samples were prepared as described.³⁴ Briefly, the samples were digested in concentrated trace-metal-grade nitric acid (final concentration 5%) overnight in a 70 °C oven, sealed in conical screw-top tubes with an electrical tape wrapped around the seal. If the samples were cells or organelles, hydrogen peroxide [final concentration 2.5% (v/v)] was added to cooled samples, which were then incubated for 1 h at 70 °C. The cooled samples were diluted with HPW to 5 or 10 mL final volume and autoinjected into the ICP-MS.

Respirometry. Isolated mitochondria (5-10 mg) were pelleted anaerobically and stored on ice. Respirometer (Oroboros O2K) chambers were washed 3× with ETOH, 3× with aerobic water, and 1× with aerobic respirometry buffer before being filled with respirometry buffer (20 mM HEPES pH 7.4, 0.6 M mannitol, 1 mM EGTA, and 0.2% wt/vol BSA). The chambers were sealed with Peek stoppers and incubated for 30 min until O2 levels were stabilized. The pelleted mitochondria were resuspended in 1.0 mL of respirometry buffer, and then 0.025-0.100 mg of the suspended mitochondria was injected with a Hamilton syringe into the respirometry chamber. Sodium succinate (5 mM), disodium ADP (2 mM) and potassium phosphate (4 mM), antimycin A (1 μ M), sodium ascorbate and TMPD (1 mM each), and KCN (5 μ M; all final) were added sequentially, with sufficient time between each addition for the O₂ consumption rate to stabilize.

Confocal Microscopy. A suspension of isolated mitochondria was incubated on ice with 100 nM Mitotracker (Molecular Probes) for 10 min before being added to a slide pretreated with poly-L-lysine. Coverglass no. 1.5 was applied and sealed with clear nail polish. Confocal imaging used a Leica SP8 confocal microscope equipped with a HC PL APO CS2 100×/1.40 oil immersion objective, hybrid detectors, and a white light laser. The excitation wavelength was 578 nm, and the emission wavelengths were 586-652 nm. Image z-stacks were acquired using the Lightning wizard in the LASX software (ver.

3.5.5), with a pinhole size of 0.84 AU, line averaging (n = 2), a voxel size of $51 \times 51 \times 234$ nm, and default processing parameters in the Lightning deconvolution module.

RESULTS

We had four objectives for this study. First, we wanted to determine whether aqueous FeII could be imported into intact mitochondria. Second, if so, we wanted to determine whether the imported iron could be incorporated into mitochondrial iron-containing proteins and under what conditions. Third, we wanted to determine whether a LMM iron-containing species was exported from intact mitochondria. Fourth, we wanted to determine whether mitochondrial iron could be incorporated into cytosolic proteins. Figure 1 provides an overview of the study and our approach.

We first isolated mitochondria and assessed their purity by western blot using antibodies against mitochondrial porin, vacuolar CPY, cytosolic protein PGK, and endoplasmic reticulum (ER) protein Kar2 (Figure 2A). The two batches whose blots are shown were significantly enriched in porin relative to the enrichment of whole cell lysates. Isolated mitochondria were not noticeably contaminated by vacuoles and cytosol, as monitored by CPY and PGK blot intensities, respectively. Endoplasmic reticulum as monitored by Kar2 was a minor contaminant. This was not surprising as mitochondria and ER interact.³⁵ Six different western blots with one to two batches per blot were obtained in the study, all giving similar results.

Isolated mitochondria exhibited a membrane potential as revealed by the confocal fluorescence microscopic images of mitotracker-treated organelles (Figure 2B). The potential was abolished when the decoupler CCCP was added. The isolated mitochondria exhibited high O2 consumption activity (Figure 2C). Upon adding succinate, the rate of O2 consumption increased due to the flow of reducing equivalents through the ETC. The rate of O₂ consumption declined after adding antimycin A, an inhibitor of respiratory complex III. Subsequent addition of TMPD (an artificial substrate for respiratory complex IV (RCIV)) and the reductant ascorbate increased O2 consumption, indicating RCIV activity. Subsequent addition of KCN, an inhibitor of RCIV, abolished O₂ consumption, again as expected. Similar results were obtained using three additional batches of mitochondria (Figure S1).

Interestingly, the observed substrate-dependent O2 consumption pattern differed from that of aerobically isolated mitochondria. The anaerobically isolated mitochondria exhibited O₂ consumption upon addition of succinate alone (Figures 2C and S1), while traditional mitochondrial respirometry requires both succinate and ADP for activity to develop.³⁶ This may have arisen because in anoxia, mitochondrial ATPases function in reverse, hydrolyzing ATP to ADP to maintain a proton gradient.³⁷ Thus, there might be an abundance of ADP in anaerobically isolated mitochondria such that only succinate is required to stimulate O2 consumption activity.

Mitochondrial Iron Import/Export Assay. We modified the (Fe-S)_{int} assay of Pandey et al. to directly detect exported iron by LC-ICP-MS. The assay was performed anaerobically in a refrigerated glovebox using fresh mitochondria immediately after isolation. Radiolabeled cysteine was replaced with a 10× higher concentration of unlabeled cysteine.

The components of our assay routinely contained significant levels of contaminating natural abundance iron (92% ⁵⁶Fe,

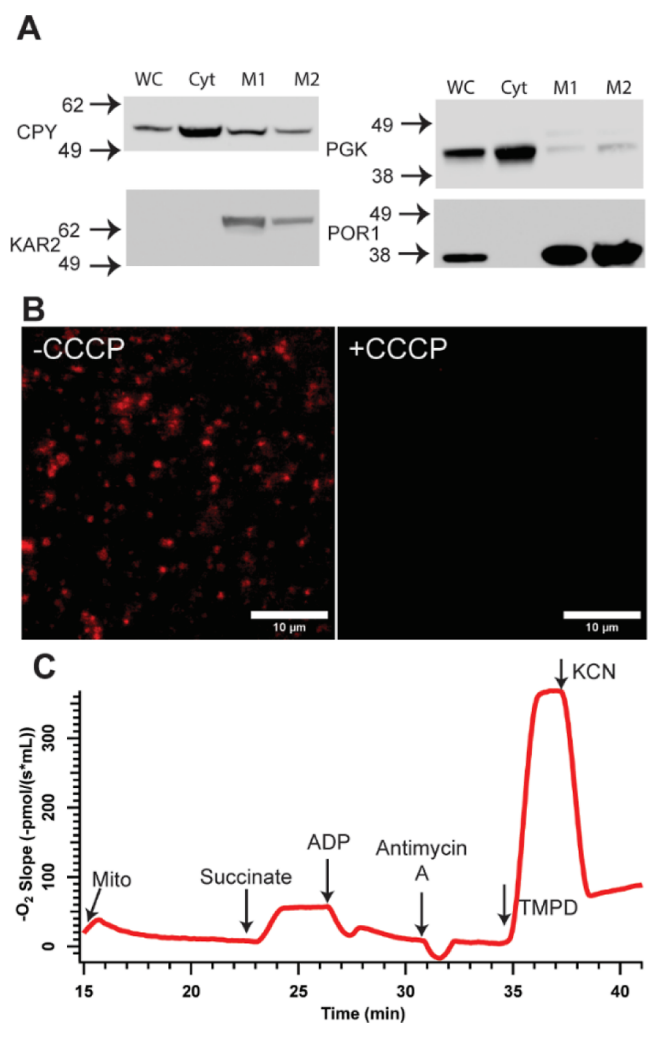


Figure 2. Characterization of isolated mitochondria: Panel (A): Western blot of isolated mitochondria. Left to right lanes: WC (whole cell sample), Cyt (isolated cytosol), M1 (gradient-purified isolated mitochondria), and M2 (equivalent mitochondria from another batch). Numbers on the left indicate masses of molecular markers. Antibody staining: CPY, vacuolar carboxypeptidase Y; KAR2, endoplasmic reticula protein; PGK, cytosolic phosphoglycerate kinase; POR1, mitochondrial porin. 30 μ g of protein was added per well. Panel (B): Confocal microscopic images of untreated mitochondria labeled with a mitotracker without (left) and with CCCP (right). Panel (C): Rate of O₂ consumption vs time using 25 μ g of isolated mitochondria. Added components were (in final concentrations) 5 mM succinate, 2 mM ADP, 4 mM phosphate, 1 μ M antimycin, 1 mM each ascorbate and TMPD (tetramethyl-p-phenylenediamine dihydrochloride), and 5 μ M cyanide.

5.8% ⁵⁴Fe, and 2.1% ⁵⁷Fe). The ATP used in the activation cocktail was especially contaminated. To distinguish contaminating iron from that of interest, mitochondria were isolated from the cells grown in media enriched in ⁵⁷Fe, and then the ⁵⁷Fe isotope was monitored by ICP-MS. Furthermore, we incubated ⁵⁷Fe-enriched mitochondria with ⁵⁴Fe^{II} ascorbate (in *BF* buffer) to monitor iron "loading". We also monitored ⁵⁶Fe in LC runs but used those results only to estimate the contaminating ⁵⁴Fe contribution which was then subtracted from overall ⁵⁴Fe intensities. To do this, we multiplied the intensity of the observed ⁵⁶Fe trace by the ⁵⁴Fe/⁵⁶Fe intensity ratio as obtained from a separate injection of a standard natural abundance iron solution. Then, we subtracted the resulting

intensity-adjusted ⁵⁶Fe trace from the observed ⁵⁴Fe trace to reveal the ⁵⁴Fe intensity arising exclusively from intentionally added ⁵⁴Fe. This strategic use of isotopes allowed us to distinguish mitochondrial (⁵⁷Fe), loaded (⁵⁴Fe), and contaminating (⁵⁶Fe) iron.

Typically, a pellet of ⁵⁷Fe-enriched mitochondria was resuspended in either buffer *B, BF, BAC, Bcyt,* or *BACcyt.* Buffer *B* served as a negative control. Buffer *BF* was used to load mitochondria with ⁵⁴Fe, *BAC* was used to stimulate mitochondrial ISC assembly, and *BACcyt* was used to do the same within cytosol. ^{31,38} After incubation, reactions were halted by pelleting the mitochondria via centrifugation and separating the supernatant. Supernatants (a.k.a. post-incubation buffers) were analyzed by LC-ICP-MS. Post-incubation mitochondria were lysed with a detergent, and the resulting SMEs were separated into retentates and FTS. Depending on the experiment, either or both fractions were subjected to LC-ICP-MS chromatography. The Superdex 200 and 200 Increase columns were used for retentates, and the Superdex Peptide or 30 Increase column was used for FTSs.

Iron Adsorption to and Import into Mitochondria. To address our first objective, 57 Fe-enriched mitochondria were incubated in BF buffer. This step was monitored from two perspectives, namely, from the loss of 54 Fe from the buffer and from the gain of 54 Fe into the mitochondria. In six independent experiments, 54 Fe in BF buffer declined when incubated with mitochondria (Figures 3 and S2). In the experiment of Figure 3, left panel, BF buffer was incubated with mitochondria anaerobically at -5 °C for 0, 10, and 20 min. The chromatogram of preincubation buffer BF (Figure 3, left panel, A) displayed a broad 54 Fe peak in the LMM region. This peak comigrated with a standard composed of dilute acidic

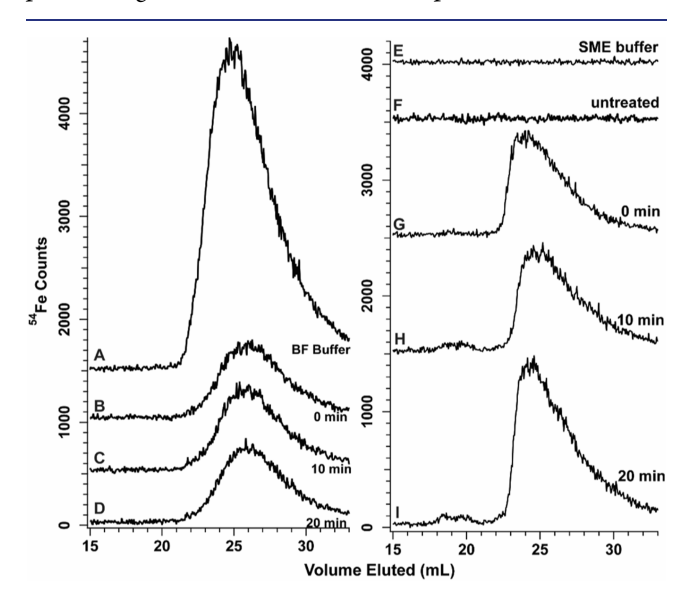


Figure 3. ⁵⁴Fe-detected LC-ICP-MS chromatograms of BF buffer (2 μ M ⁵⁴Fe) before and after incubation with ⁵⁷Fe-enriched mitochondria (15 mg). Left panel: (A) BF buffer prior to incubation; (B–D) same as (A) but 0, 10, and 20 min post-incubation. Right panel: (E) buffer used to generate SMEs; (F) FTS of SME from the mitochondria before treating with BF buffer; (G–I) FTSs from SMEs generated from the mitochondria incubated for 0, 10, and 20 min in buffer BF. Traces in right and left panels were from the same experiment, except for the untreated sample which was from another experiment. Samples were injected onto the Superdex Peptide column.

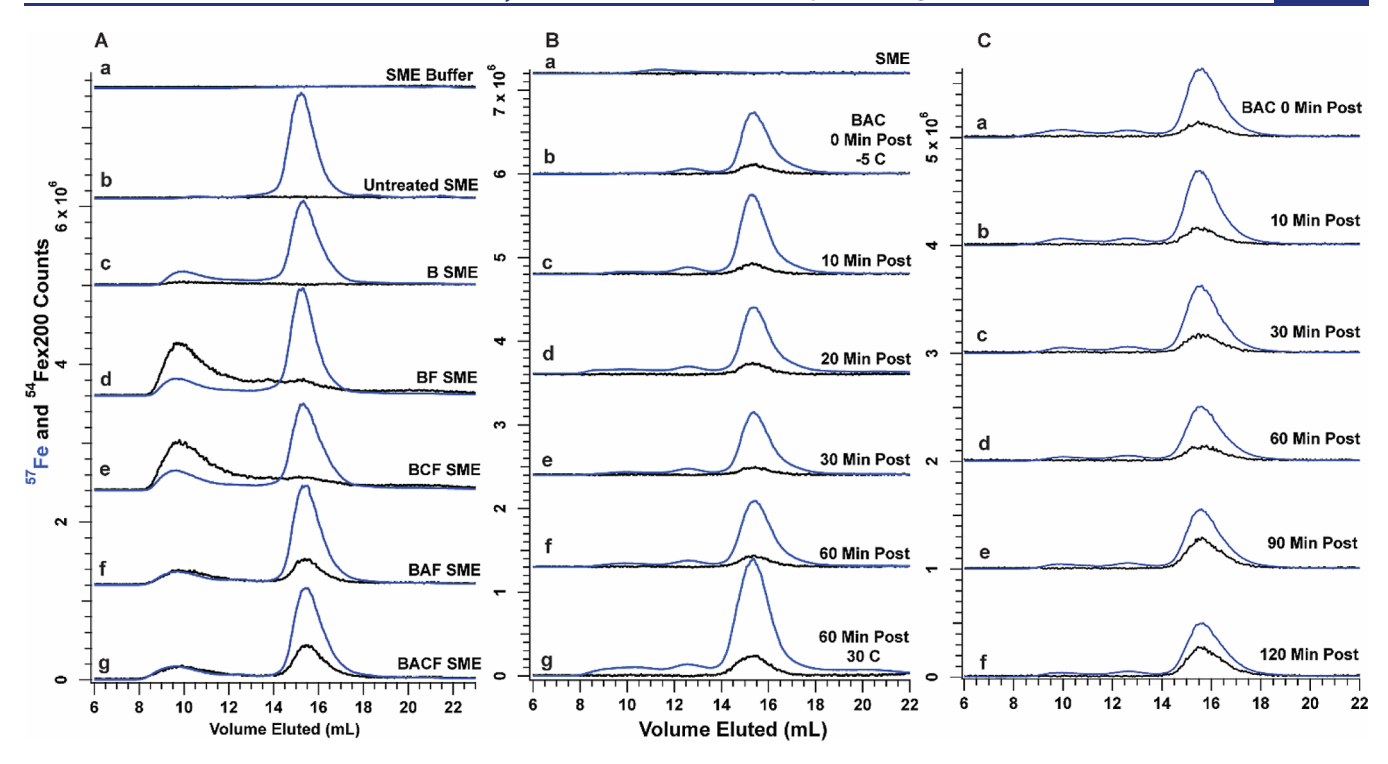


Figure 4. Chromatograms of SME retentates from ⁵⁷Fe-enriched and ⁵⁴Fe-loaded mitochondria showing incorporation of ⁵⁴Fe into mitochondrial proteins. Color coding for all figures: ⁵⁷Fe (blue) and ⁵⁴Fe (black). SMEs (500 μL) were concentrated to ~100 μL using a 10 kDa Centricon and then diluted to 500 μL with HPW. SME retentates were filtered through a 0.2 μm filter before being run on a Superdex 200 (high-mass) column. Panel (A): Incorporating aqueous ⁵⁴Fe^{II} into mitochondrial proteins requires activation components. (a) Buffer used to generate SMEs (20 mM ammonium acetate pH 6.5 + 2% Triton x-100); (b) SME retentate from the untreated ⁵⁷Fe-enriched mitochondria; (c) same as (B) except the mitochondria were treated with buffer B (30 min; 30 °C; same for all subsequent traces unless noted); (d) same as (c) except the mitochondria were treated with buffer BF; (e) same as (d) except treated with buffer BCF (BF + 100 μM cysteine); (f) same as (d) except treated with buffer BAF (BF + A activation components); and (g) same as (d) except treated with buffer BACF (BF + AC activation components). Observed ⁵⁴Fe traces were corrected assuming a ⁵⁴Fe/⁵⁶Fe ratio of 0.65% rather than 1.7%, which was used for other traces. Panel B: Temperature dependence of iron incorporation into mitochondrial proteins: (a) SME buffer and (b) from the mitochondria incubated in BAC buffer for 0 min at −5 °C. (c−f) Same as (b) but incubated for 10, 20, 30, and 60 min, respectively and (G) from the mitochondria incubated in BAC buffer for 0, 10, 30, 60, 90, and 120 min, respectively.

⁵⁴Fe^{III} plus excess ascorbate. The Mössbauer spectrum of a similarly prepared ⁵⁷Fe standard exhibited a quadrupole doublet with parameters typical of aqueous high-spin Fe^{II}. Thus, we will describe ⁵⁴Fe in *BF* buffer as "aqueous ⁵⁴Fe^{II"}. The broadness of this peak is due to the interaction of aqueous Fe^{II} with the column.³⁹

The intensity of the aqueous $^{54}\text{Fe}^{II}$ peak in traces from all the three post-incubation supernatants was $\sim\!26\%$ of the preincubation buffer intensity (Figure 3, left panel, B–D). This suggested that even at -5 °C, the mitochondria-dependent decline in ^{54}Fe concentration was complete at "0 min", which included a 12 min deadtime required to halt the reaction. At 30 °C, the optimal growth temperature of *S. cerevisiae*, the mitochondria-dependent decline of ^{54}Fe would undoubtedly occur faster.

The decline of iron concentration from preto post-incubation buffers was unaffected by adding 5% O_2 to the assay or by adding 50 μ M CCCP to oxygenated samples (Figure S3). These results suggested that a membrane potential was not required for the incorporation of aqueous Fe^{II} into the mitochondria. Another reasonable possibility is that most of the added iron adhered to the organelle in a CCCP-independent manner, but that the small fraction that entered the organelle was CCCP dependent but undetected in our experiment.

To assess whether the decrease of 54 Fe in post-incubation supernatants was due to iron adsorbing on the column, the samples were injected onto a "ghost" column in which the real column was replaced with Peek tubing. In the experiment of Figure S2A, $10~\mu\text{M}$ 54 Fe was included in BF buffer (top group), while in another, $2~\mu\text{M}$ 54 Fe was included (bottom group). In both cases, the 54 Fe peak intensity declined within the processing deadtime and then plateaued for the duration of the experiment. Thus, the observed decline was not due to iron adsorption onto the column. The iron concentrations in the 2 and $10~\mu\text{M}$ preincubation BF buffers were determined to be 2.2 and $12~\mu\text{M}$, respectively (including contaminating iron); post-incubation samples contained \sim 0.7 and \sim 1.6 μM Fe, respectively (Table S3).

A 85% decline of 10 μ M ⁵⁴Fe in 1.5 mL of buffer corresponds to ~12 nmoles ⁵⁴Fe. That iron was either imported and/or surface-adsorbed by the mitochondria (15 mg of protein). "Neat" mitochondria contain ~85 mg/mL mitochondrial protein, ^{30,40–42} which suggests that ~180 μ L of the mitochondria were used in the assay and that they imported or adsorbed ~70 μ M ⁵⁴Fe. Mitochondria from iron-replete WT cells contain ~750 μ M Fe, ^{30,40–42} suggesting that the ⁵⁴Fe loading process increased the iron content of the organelle by ~ 9%. We caution that these are crude approximations.

We initially considered that 54 Fe which remained in the buffer post-incubation (in the plateau region) reflected the cessation of mitochondrial iron import once the capacity of an internal iron pool had been exceeded. Accordingly, we expected that a greater percentage of 54 Fe would decline after treating mitochondria with a lower concentration of 54 Fe (e.g., 2 rather than $10~\mu\text{M}$ 54 Fe $^{\text{II}}$). Surprisingly, this expectation was not realized (Figure S2, left panel); a greater percent declined when $10~\mu\text{M}$ Fe was used. In three earlier experiments, the samples were incubated for 15 min at 30 °C. In two of those, nearly all added 54 Fe disappeared (Figure S2C,D). In the third, a significant residual intensity remained (Figure S2E). Further studies are needed to determine whether the proportion of iron remaining in these experiments might be temperature dependent.

We investigated the same process from the perspective of the mitochondria. Post-incubation mitochondria were washed with *B* buffer to remove any excess iron, and then they were used to generate SMEs. SMEs were separated into retentate and FTSs using a 10 kDa centrifugal filter. SMEs prepared from ⁵⁴Fe-loaded mitochondria exhibited a broad LMM ⁵⁴Fe LC peak that was absent in untreated mitochondria or in the SME buffer used in the experiments (Figure 3, right panel). Two other experiments displayed a similar LMM ⁵⁴Fe peak in post-incubation FTSs (Figure S4, panels A and B).

We used a ghost column to confirm that 54 Fe in this type of experiment was not adhering to the column (Figure S4, panel C). 54 Fe peaks were evident in the 0 min sample but did not increase at later times. The SME from an experiment in which the mitochondria were incubated with 10 μ M 54 Fe had 3× more iron than when incubated with 2 μ M 54 Fe. ICP-MS of SMEs obtained from two batches of mitochondria that had been treated with 10 μ M 54 Fe had \sim 3 and \sim 8 μ M 54 Fe, corresponding to \sim 0.3 and \sim 1% of total iron in the organelle. These estimates are 10–30× less than estimated from the loss of 54 Fe from the buffer. We suspect that a large portion of the 54 Fe which declined adhered to the mitochondrial surface and that portion was removed during washing. Alternatively, some mitochondria may not have lysed during SME preparation.

In summary, the iron content of buffer that initially contained 2 or 10 μ M aqueous Fe^{II} declined to about ~75% of their initial concentration when mixed with the mitochondria for ~12 min at ~5 °C (essentially deadtime). The mitochondria-dependent decline did not require activation components ATP, GTP, NADH, and cysteine nor did it require O₂. The decline would undoubtedly occur faster at 30 °C. The mitochondria either imported ⁵⁴Fe from the buffer or adsorbed it onto their surface only to release it in a soluble form during the preparation of SMEs. An order-of-magnitude calculation suggested that when 10 μ M ⁵⁴Fe was used in the assay, ~9% of total mitochondrial iron was imported or adsorbed. Of that, only a fraction was detected in the washed mitochondria, suggesting significant ⁵⁴Fe weakly bound to the surface

Loaded ⁵⁴Fe Was Installed into Mitochondrial Proteins When ISC Assembly Was Stimulated. In addressing our second objective, we reasoned that if some ⁵⁴Fe had been imported into the mitochondrial matrix, it might be used in ISC assembly and thus become incorporated into mitochondrial ISC proteins. To investigate, we incubated ⁵⁷Fe-enriched mitochondria with buffers known to activate ISC assembly (and others with control buffer). We then isolated the organelle, prepared SMEs, and injected the retentate

fraction onto a "high mass" LC column to detect ironcontaining proteins. ISC assembly in the mitochondria is stimulated by incubating with an activation cocktail that includes ATP, GTP, NADH, Mg acetate, potassium acetate, and cysteine.³¹

Soluble iron-containing proteins from SMEs from untreated ⁵⁷Fe-enriched mitochondria eluted as a broad peak between 14 and 18 mL (Figure 4A(b)). The peak was absent in the SME buffer (Figure 4A(a)). A similar result was obtained with the mitochondria treated with *B* buffer (Figure 4A(c)). The inclusion of O₂ had no noticeable effect (Figure S5D,E). The intensity of the ⁵⁷Fe peak was virtually constant for each condition tested in the experiment of Figure 4 and thus served de facto as an internal standard. Although the peak appeared Gaussian, multiple unresolved ⁵⁷Fe-enriched proteins likely contributed to it; calibration using proteins of known molecular weight indicated an apparent mass range traversing the peak between approximately 120–20 kDa. Over 80% of mitochondrial iron-containing proteins contain ISCs or heme groups, with masses within this range. ¹²

There was a slight 54 Fe peak in the SMEs from mitochondria treated with BF (2 μ M 54 Fe) buffer (Figures 4Ad and SSB). The 54 Fe peak intensity was similar when cysteine was included (Figure 4A(e)). The 54 Fe peak intensity was significantly greater when the mitochondria were treated with BF buffer + activation cocktail (Figure 4A(f)) and most intense when treated with both the activation cocktail and cysteine (BAC buffer) (Figures 4A(g) and S5C,E). Some 57 Fe and 54 Fe traces additionally exhibited a broad peak at \sim 9.5 mL, near the void volume. This high-mass peak could have originated from a protein or from an Fe aggregate/nanoparticle.

Using the *BAC* buffer to activate ISC assembly, we examined the kinetics of this process. At -5 °C, the intensity of the ⁵⁷Fe and ⁵⁴Fe peaks at 15 mL elution volume increased marginally over a 60 min incubation (Figure 4B(a-f)). However, the intensity increased 2-fold in matched samples at 30 °C (Figure 4B(g)). At that temperature, ⁵⁴Fe incorporation into mitochondrial proteins increased during a 120 min incubation (Figure 4, panel C). These experiments were repeated twice with similar results (Figures S6 and S7).

In summary, these experiments demonstrated that some ⁵⁴Fe that was loaded into ⁵⁷Fe-enriched mitochondria became incorporated into mitochondrial iron-containing proteins, but only when ISC assembly was activated. Thus, at least some of the added aqueous ⁵⁴Fe^{II} was imported into the organelle and did not adhere to its surface. We speculate that the imported ⁵⁴Fe contributed to an existing ⁵⁷Fe^{II} pool in the matrix, and that this pool, containing both isotopes, served as a feedstock for ISC assembly. Although we could not quantify the rate of this process, the incorporation of iron from this pool into mitochondrial iron-containing proteins was significantly slower than aqueous Fe^{II} import into the organelle (since peaks developed over 1–2 h at 30 °C).

Low-Molecular-Mass Iron Was Exported from Mitochondria When ISC Assembly Was Stimulated. To address the third objective of the study, we loaded ⁵⁷Fe-enriched mitochondria with ⁵⁴Fe. We washed the organelle to remove excess ⁵⁴Fe and incubated the loaded mitochondria in either *BAC* buffer, to stimulate ISC activity, or *B* buffer as a negative control. After increasing the incubation times, we centrifuged the suspensions and injected supernatants onto a low-mass LC column to monitor time-dependent increases in LMM ⁵⁴Fe and/or ⁵⁷Fe peaks.

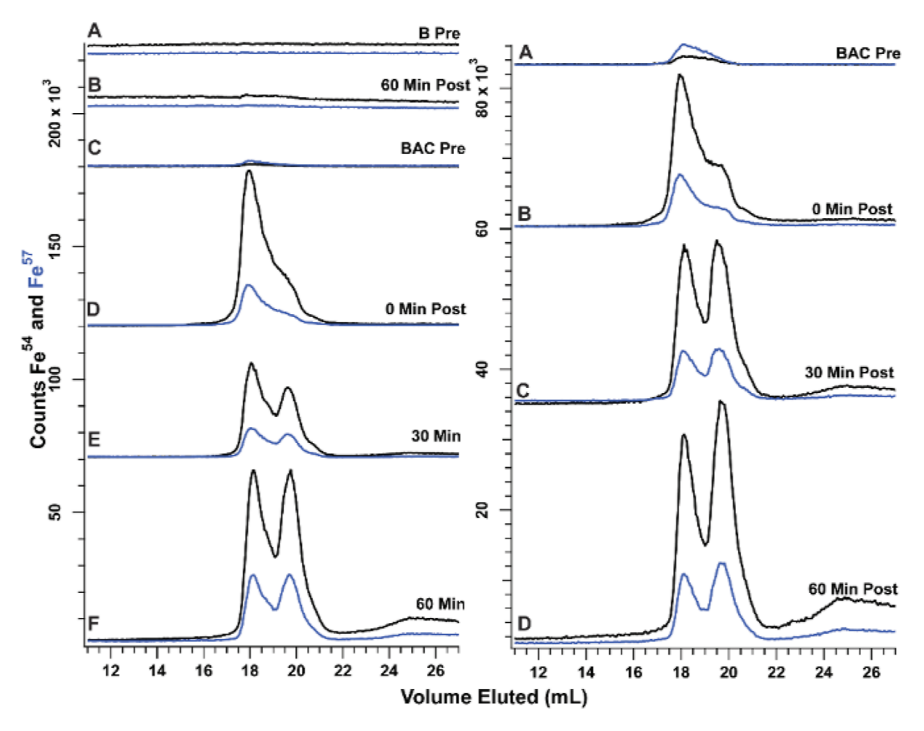


Figure 5. 54 Fe and 57 Fe chromatograms of supernatants before and after 54 Fe-loaded and 57 Fe-enriched mitochondria were incubated in *B* or *BAC* buffers and then separated. 57 Fe-enriched mitochondria were pretreated with *BF* buffer (10 μ M 54 Fe) for 15 min at 30 $^{\circ}$ C and then washed 1× before resuspending in buffers *B* or *BAC*. Left panel: Mitochondria isolated from aerobic respiring cells. (A) Buffer *B* and (B) same as (A) but incubated with 54 Fe-loaded and 57 Fe-enriched mitochondria for 60 min at 30 $^{\circ}$ C and then separated by a 10 min 12,000g spin down. (C) Buffer *BAC*. (D–F) are the same as (C) but incubated in 54 Fe-loaded and 57 Fe-enriched mitochondria for 0, 30, and 60 min at 30 $^{\circ}$ C and then separated as described above. Right panel: Mitochondria isolated from hypoxic fermenting cells. (A) Buffer *BAC*. (B–D) Supernatants after mitochondrial incubation for 0, 30, and 60 min, respectively, and then separation by spin down. All samples were passed through a 0.2 μ m filter before being run on a Superdex 30 Increase (low-mass) column at 0.6 mL/min.

In one experiment, we used ⁵⁷Fe-enriched and ⁵⁴Fe-loaded mitochondria that had been isolated from aerobic respiring cells. No LMM Fe peaks were obtained after a 60 min incubation in B buffer (Figure 5, left panel, A and B), but 2 Fe peaks were observed when BAC buffer was used, including one at 18 mL and the other at 19.5 mL (Figure 5, left panel, C-F). The intensity of the latter peak increased over a 60 min incubation period whereas that at 18 mL remained approximately constant. Both 54Fe (black) and 57Fe (blue) exhibited the same behavior. A second experiment using ⁵⁷Feenriched and ⁵⁴Fe-loaded mitochondria from fermenting cells exhibited similar results (Figure 5, right panel). We concluded from these and earlier studies (Figures S8-S11) that two LMM iron species were exported from intact mitochondria, but only when ISC assembly activity in the mitochondria was stimulated by AC. The LMM Fe species at 18 mL developed fully within the 12 min deadtime of the experiment, whereas the 19.5 mL species developed over the course of 60 min at 30 °C. In Figure 5, a third broad peak at ~25 mL is evident, which probably reflected aqueous or weakly bound Fe. Whether the two dominant species were exported from the matrix or from the mitochondrial surface is uncertain. Also uncertain is whether two distinct complexes were exported or if a single species was exported after which portions became coordinated by different ligands to generate the two major peaks.

In two batches, we quantified the concentration of iron exported from AC-activated mitochondria, obtaining $\sim 1~\mu M$ for one batch and $\sim 9~\mu M$ for the other (Table S4). Calculations were like those described previously for iron import, but they also involved subtracting the background iron

in B buffer and summing 54 Fe and 57 Fe contributions. The resulting concentrations corresponded to 1 and $\sim 10\%$ of total mitochondrial iron, respectively. Previous studies have suggested that the labile Fe^{II} pool in the mitochondria represents 3–20% of the total mitochondrial iron content, depending on the carbon source used in the growth media. These numbers seem similar, suggesting that the LMM Fe species originated from this pool, but further studies are needed to confirm this.

Earlier experiments exhibited similar results except that the two low-mass Fe peaks were less well resolved, and their elution volumes were slightly shifted due to differences in column conditions (Figures S8–S11). The experiments of Figure S8 show that the activation components were required for these peaks to develop (left panel), and they revealed that the kinetics of the process was slower at -5 °C than at 30 °C (right panel). Qualitatively, the rate of this process (export of LMM Fe species) was slower than Fe import and comparable to the rate of incorporating loaded ⁵⁴Fe into mitochondrial ISCs.

Both ⁵⁴Fe and ⁵⁷Fe traces exhibited similar—even parallel—behavior in the region containing the two major peaks. This implied that the exported iron originated from a common pool of mitochondrial iron, to be referred to as the "entry" pool, that contained both loaded ⁵⁴Fe and pre-existing ⁵⁷Fe.

Careful inspection of the traces in Figure S8 show that some minor ⁵⁷Fe peaks were observed at lower elution volumes (indicating higher mass species including proteins and iron aggregates/nanoparticles)—but intriguingly without parallel ⁵⁴Fe peaks (see Figure S8, left panel, D and F and right panel,

trace G). These high-mass ⁵⁷Fe peaks appeared when the mitochondria were incubated in BAC buffer but not in B buffer. The same effect was observed with greater clarity in the experiment of Figure S9. Using BAC buffer to stimulate export, the same LMM ⁵⁴Fe and ⁵⁷Fe peaks developed over 120 min incubation. During that period, an intense ⁵⁷Fe peak developed in a time-dependent fashion in the high-mass region-but no parallel ⁵⁴Fe peak developed (see traces $C \rightarrow G$). Also, the rate at which the high-mass 57Fe peak developed seemed to increase with time. One explanation is that the mitochondria degraded during incubation in AC, releasing high-mass forms of pre-existing ⁵⁷Fe in the process but not ⁵⁴Fe and ⁵⁷Fe from the entry pool. How such a selective release might happen is difficult to envision. Alternatively, the intact AC-activated mitochondria may have exported a 57Fe species from a preexisting "established" pool that contained mostly ⁵⁷Fe. The exported species may have been a HMM protein or a LMM species that aggregated during the time between sample collection and analysis.

The same type of experiment was analyzed from the perspective of the mitochondria; we anticipated a decline of a LMM iron species (from the entry pool). SMEs were prepared using post-incubation mitochondria, and the FTSs were analyzed by LC-ICP-MS. The intensity of the LMM iron species in the SMEs indeed declined after treatment with *BAC* buffer (Figure S4Bf-k), consistent with the export of Fe from the mitochondria.

To characterize the two exported LMM Fe species, we compared their elution volumes to those of various candidate Fe standards. Activation buffer contained ATP, GTP, NADH, and cysteine, all potential ligands to iron. We prepared iron complexes by mixing 2 μ M FeSO₄ with each of these potential ligands and then injected the solutions onto the low-mass 30 increase column. In a recent study, we prepared an Fe-ATP complex³⁹ and found using Mössbauer spectroscopy that the complex was oxidized to Fe(III)ATP unless reductants dithionite, ascorbate, or glutathione were included. The elution volume of the Fe-ATP standard was slightly greater than that of Fe-GTP and was not significantly altered by the oxidation state.

In the current study, Fe-ATP nearly comigrated with the "fast-developing" LMM Fe species that was exported from intact mitochondria in an AC-dependent fashion (Figure 6, B vs F). Solutions in which FeSO₄ was mixed with cysteine and NADH exhibited no Fe peaks (Figure 6D,E) are consistent with previous results.³⁹ The absence of Fe peaks in the traces of Figure 6D,E arose because aqueous Fe^{II} adsorbed onto the 30 Increase column. None of the components of *BAC* buffer comigrated exactly with the "slow-developing" Fe species that was exported from the mitochondria upon AC activation. This implied that the "slow-developing" LMM Fe species was not a complex involving the activation ligands (though a combination of those ligands cannot be excluded).

Also noteworthy was that a P-detected peak developed in parallel with the slow-developing species, and it comigrated exactly. No comigrating peak was evident in the S trace. This suggested that the slow-developing LMM Fe species had a P-containing ligand but not a S-containing one (we caution that S and P detection by our ICP-MS is less sensitive than that of Fe, which could complicate the analysis).

We also performed a control experiment in which ⁵⁴Fe was added to BAC buffer in the absence of mitochondria. As expected, the Fe-ATP complex formed (Figure S12). A second

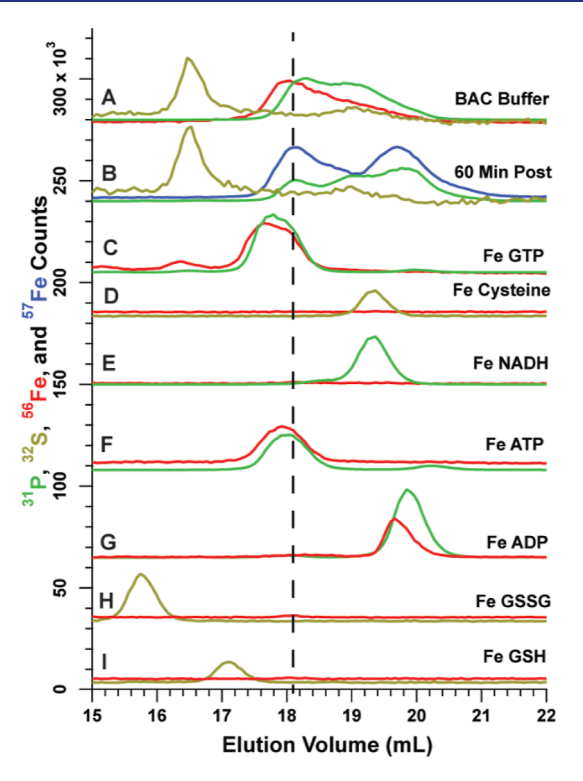


Figure 6. LC-ICP-MS chromatograms of candidate iron standards: (A) *BAC* buffer and (B) same as (A) except incubated with 54 Feloaded and 57 Fe-enriched mitochondria as in Figure 5 for 60 min at 30 $^{\circ}$ C and then separated. All standards were prepared with 2 μ M FeSO₄ + 1 mM (final concentrations) of the following ligands; (C) GTP; (D) cysteine; (E) NADH, (F) ATP; (G) ADP; (H) GSSG; and (I) GSH. Traces A and B are from Figure 5 left traces C and D, and trace F is from ref 39. Intensities have been scaled for improved visualization. Color coding: 31 P (green), 32 S (gold), 56 Fe (red), and 57 Fe (blue). Samples were run on a Superdex 30 Increase column.

Fe species also formed at an elution volume similar to (but not the same as) the "slow-developing" species observed in standard assays. The corresponding phosphorous traces exhibited two peaks, suggesting that both species in the control were nucleotide phosphates (e.g., ATP, ADP, and GTP).

Mitochondrial Iron Was Incorporated into Cytosolic Proteins. The fourth and final objective of this study was to determine whether exported mitochondrial iron could become incorporated into cytosolic iron-containing proteins, and if so, the conditions for that export. To address this, we isolated cytosol in *B* buffer from cells grown using natural abundance unenriched iron. To that was added either nothing (*Bcyt*) or *AC* powders (*BACcyt*). The resulting solutions were incubated with ⁵⁷Fe-enriched and ⁵⁴Fe-loaded mitochondria. After increasing the incubation times at 30 °C, we isolated postincubation solutions by centrifugation, concentrated them with a 10 kDa cut-off membrane, and then injected the retentates onto the high-mass column. ⁵⁷Fe, ⁵⁴Fe, ⁵⁶Fe, and absorbance at 420 nm (A420) were monitored simultaneously. A420 is associated with the brown color of ISCs and heme centers.

In three independent experiments in which cytosol was mixed with *BAC* buffer, ⁵⁷Fe became incorporated into iron-containing cytosolic proteins over 60–120 min (Figure 7). In each experiment, four distinguishable ⁵⁷Fe peaks developed, with matching A420 peaks for three of them. From left to right, we labeled these peaks HM (high mass), NA (no A420), MA

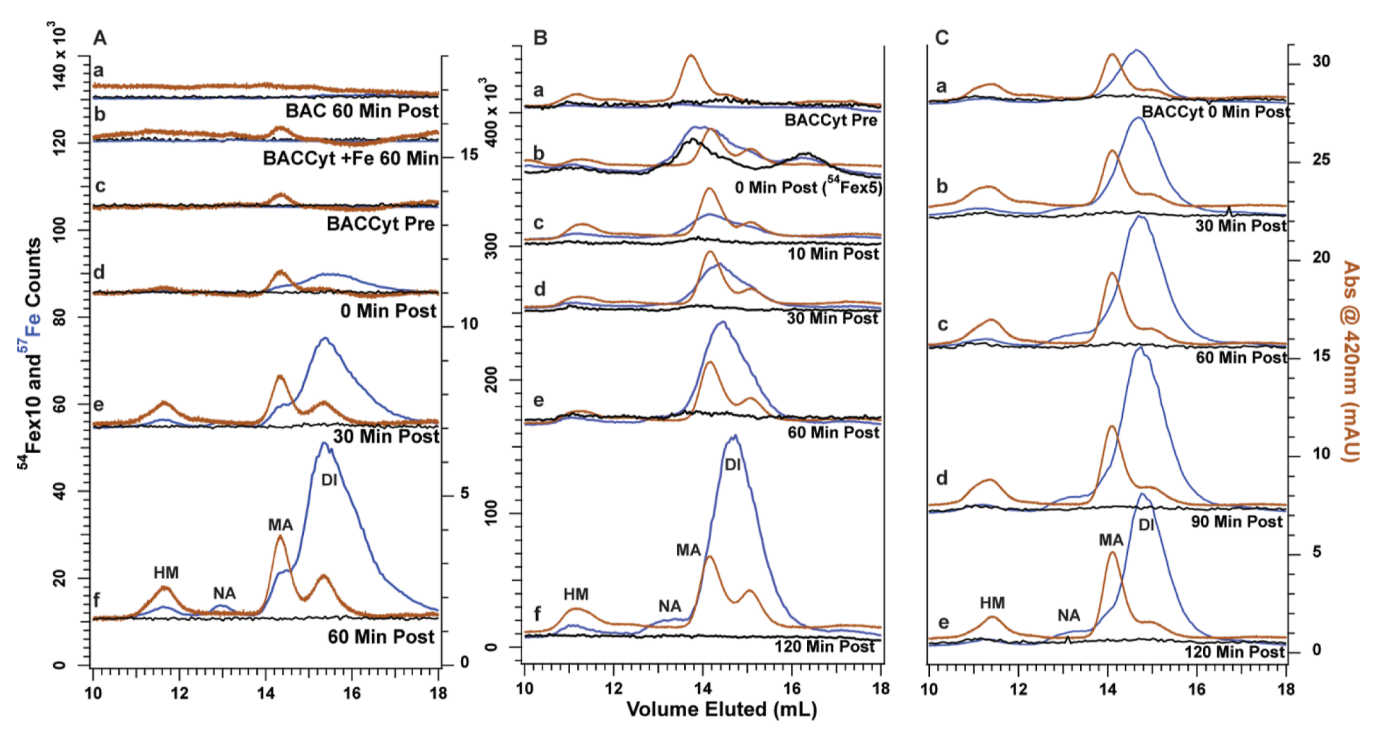


Figure 7. Incorporation of mitochondrial ⁵⁷Fe into cytosolic proteins: ⁵⁴Fe-loaded and ⁵⁷Fe-enriched mitochondria were incubated in *BACcyt* buffer at 30 °C for 0–120 min. After incubation, the supernatants (1.5 mL) were concentrated to 500 μL using a 10 kDa Centricon, and retentates were passed through a 0.2 μm filter and injected in a Superdex 200 Increase (high-mass) column. Color coding as in other figures except A420 (brown line). Left panel A: (a) *BAC* buffer post 60 min of incubation with mitochondria; (b) *BACcyt* buffer + 2 μM ⁵⁴Fe without mitochondria for 60 min; (c) *BACcyt* buffer (containing 0.75 mg/mL cytosolic protein); (d) same as (c) but incubated with ⁵⁴Fe-loaded and ⁵⁷Fe-enriched mitochondria for 0 min; (e) same as (d) but for 30 min; and (f) same as (d) but for 60 min. Peaks were labeled HM (high-mass), NA (no absorption), MA (max absorption), and DI (dominant intensity). Middle panel B: (a) *BACcyt* buffer (containing 0.8 mg/mL cytosolic protein); (b) same as (a) but incubated in ⁵⁴Fe-loaded and ⁵⁷Fe-enriched mitochondria for 0 min; (c) same as (b) but for 10 min; (d) same as (b) but for 30 min; (e) same as (b) but for 60 min; and (f) same as (b) but for 120 min. Right panel C: Repeat of middle experiment. (a) *BACcyt* buffer incubated with ⁵⁴Fe-loaded and ⁵⁷Fe-enriched mitochondria for 0 min; (b) same as (a) except incubated for 30 min; (c) same as (a) but for 60 min; (d) same as (a) but for 90 min; and (e) same as (a) but for 120 min.

(max A420), and DI (dominant iron). See Table S5 for specific elution volumes. Calibration against protein standards suggested approximate apparent masses ranging between 180 and 70 kDa. There are \sim 34 iron-containing proteins in the cytosol of *S. cerevisiae*, most of which contain ISCs or hemes. We have not assigned the observed peaks to them. Interestingly, the rates at which iron was incorporated into the proteins associated with the observed peaks varied, as did the ratio of 57 Fe/A₄₂₀. Different ratios probably reflected different extinction coefficients at 420 nm. The corresponding 54 Fe peaks were not observed in the experiments of Figure 7; however, in an experiment using twice the concentration of cytosol and a longer assay time, 54 Fe peaks did develop (Figure S13).

Three important controls were performed. When buffer *Bcyt* was used instead of *BACcyt*, minimal peak intensities developed (Figure S14). This control was not "clean" because the cytosol likely contained endogenous activation components. Consistent with that, the samples made from older cytosol exhibited less incorporation into proteins, perhaps due to the hydrolysis of endogenous cytosolic nucleotide triphosphates. We attempted to deplete endogenous NTPs from cytosol by removing the low-mass species using a 3 kDa filter and washing the retentate with NTP-free *B* buffer. This treatment showed a modest reduction in the high-mass iron that was incorporated into the cytosol. Despite this complication, our results show that AC activation of ISC

assembly stimulated the incorporation of mitochondrial iron into cytosolic proteins.

The second important control was to exclude the mitochondria. In this experiment, Fe^{II} and the AC activation components were added to the cytosol, but no iron or A420 peaks developed after 60 min of incubation (Figures 7Ab and S15). This indicated that cytosolic Fe^{II}, e.g., from the labile iron pool, is not incorporated into cytosolic proteins. This reinforced our conclusion that the iron that incorporated into cytosolic proteins originated from the mitochondria.

The third and final control was to exclude the cytosol from this experiment and to confirm that mitochondria alone do not export a high-mass Fe species. In this experiment, no HMM Fe species was observed (Figures 7Aa and S16). This also indicated that the iron detected in cytosolic samples did not originate from mitochondrial degradation products.

DISCUSSION

In this study, we found that a portion of the aqueous ⁵⁴Fe^{II} that was added to isolated ⁵⁷Fe-enriched mitochondria was imported into the organelle. Another portion likely adhered to the mitochondrial exterior, consistent with earlier results. ⁴⁴ We estimate that only a few percent of total mitochondrial iron was imported, with the majority surface-bound. However, some of the imported iron was installed into mitochondrial iron-containing proteins, but only when the ISC assembly system in the organelle was activated. The imported iron likely

entered the pool used as a feedstock for ISC assembly (Figure 8). Prior to loading with ⁵⁴Fe, this "entry pool" contained pre-existing ⁵⁷Fe, consistent with both isotopes becoming installed in mitochondrial iron-containing proteins.

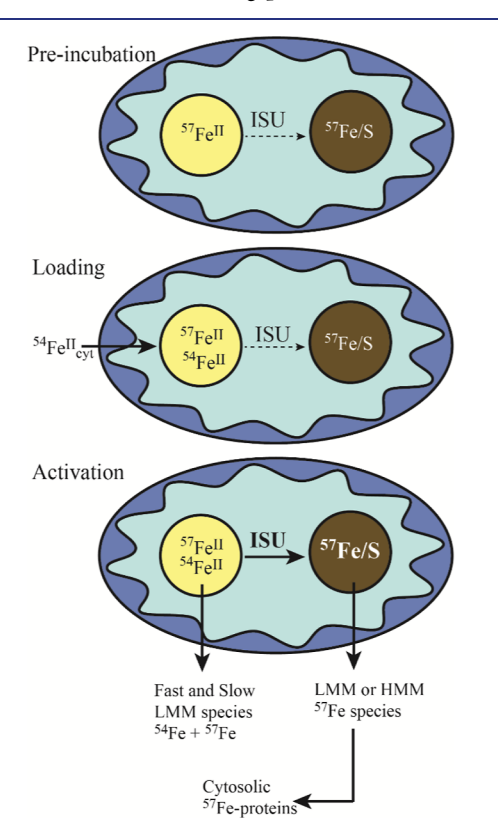


Figure 8. Working model to explain our results: The model assumes that the ⁵⁷Fe-enriched mitochondria contain two pools of dynamic iron, namely, an entry pool (yellow) and an established pool (brown). The entry pool, viewed here as located in the matrix, contains nonheme high-spin ⁵⁷Fe^{II} ions that are used as a substrate for ISC assembly. The established pool contains the products of that assembly. Most of that iron, in the form of ISCs, will ultimately be installed into apo forms of mitochondrial ISC proteins. The aqueous ⁵⁴Fe^{II} used in loading is imported quickly into the entry pool and mixes with existing ⁵⁷Fe^{II} in that pool. When the ISU system is activated (by adding the AC activation cocktail), iron from the entry pool is slowly used to generate ISCs that mix with ⁵⁷Fe ISCs in the established pool. Simultaneously, the two observed LMM ⁵⁴Fe/⁵⁷Fe species (called fast and slow) are exported into the supernatant/ buffer/cytosol. Simultaneously, an unidentified form of iron is exported from the established pool. This form of iron is installed into client ISC proteins by the CIA. The exported iron is primarily ⁵⁷Fe because the processing of ⁵⁴Fe from the entry pool is slow relative to the incubation times of our experiments.

Aqueous Fe^{II} was imported into the organelle without including any activation components or exposure to O₂, which are typically required to generate a membrane potential, nor was the process inhibited by adding the uncoupler CCCP. Import of cytosolic Fe^{II} by Mrs3/4, high-affinity iron importers on the inner mitochondrial membrane, requires a membrane potential.⁴ A membrane potential might not be required if other importers were involved.^{5,6} Another reasonable possibility is that only the small portion of added iron that was actually imported into the organelle required a membrane potential.

We also examined the import of ⁵⁴Fe^{II} from the perspective of the mitochondria. Prior to treatment, mitochondrial SMEs exhibited a low-intensity LMM ⁵⁷Fe peak which likely originated from the labile Fe^{II} pool previously described. Earlier studies in which "Fe580" was detected used EDTA in the buffers and 50 mM Tris mobile phase. For our current preparations, a smaller pool of aqueous Fe was present, perhaps because no EDTA and a different mobile phase were used. Further studies are required to investigate the composition of the labile iron pool in the mitochondria and whether it is synonymous with the entry pool suggested here.

Some mitochondrial iron, both loaded ⁵⁴Fe and pre-existing ⁵⁷Fe, was exported into the buffer or cytosol in the form of two LMM species. This process required activating the mitochondria for the synthesis of ISCs. The two species developed at different rates. The "fast-developing" species was fully developed within the 12 min deadtime of our assay, whereas the "slow-developing" species developed gradually over an hour.

The fast-developing species approximately comigrated with Fe-ATP. One possibility is that iron ions were exported from the mitochondria and immediately coordinated by the ATP present in the activation buffer. Another possibility is that a more complex iron-containing species, conceivably a cluster, was exported, but that it degraded in the time needed to process the samples, and that the released iron bound ATP. A third possibility is that surface-bound iron, not released by simple washing, was released from the organelle upon exposure to the activation components. ATP and GTP both bind Fe^{III} and Fe^{III} tightly, and they could serve as weak chelators for this process.³⁹

The slow-developing LMM Fe species did not exactly comigrate with any of the activation components. It developed in parallel with a P peak, suggesting that it was associated with a P-containing ligand. The presence of a comigrating P peak and the absence of a S peak do not support assigning it to [Fe₂S₂](GS)₄. The comparable intensity of the P peak relative to that due to free ATP suggests significant (mM) concentrations of a P-containing species. The slow-developing species comigrated approximately with Fe-ADP. One scenario is that Fe-ADP developed as ADP was generated. However, the activation buffer contained 4 mM ATP and no ADP, yet the two peaks ultimately had almost equal intensity. This scenario would require export of sufficient ADP to generate ~4 mM in the assay solution. Moreover, Fe binds ATP about 10 times more tightly than it binds ADP45 and so even higher concentrations of ADP would be required. All things considered, we find this scenario possible (recall that under anerobic conditions, the mitochondria convert ATP into ADP to maintain membrane potential) but not especially likely. Another possibility is that the actual LMM exported Fe species degraded during processing time to generate the slowdeveloping species (ISCs are generally unstable in aqueous solutions). Further studies are required to settle these intriguing issues.

The kinetics of these processes was qualitatively assessed. Iron import into the mitochondria was fastest, followed by mitochondrial ISC assembly and LMM iron export. The slowest of the examined processes was the installation of iron into cytosolic proteins.

Finally, our results demonstrate that some mitochondrial iron, when stimulated for ISC assembly, is used by the cytosol to generate ISCs which are installed into numerous cytosolic

proteins. (Our assay does not distinguish ISCs from hemes.) The majority of the iron utilized for cytosolic ISC was mostly ⁵⁷Fe, with ⁵⁴Fe only appearing when the cytosolic protein concentration was doubled and longer assay times were used. The implication is that the iron used in the assembly of cytosolic ISC originates from an "established" pool of iron that is mostly ⁵⁷Fe. This pool would differ from the "entry" pool in which newly arriving ⁵⁴Fe was mixed with pre-existing ⁵⁷Fe.

Unexpectedly, these considerations imply that the two LMM Fe species that are exported from activated mitochondria may not be used for cytosolic ISC assembly. The exported Fe species could be a HMM species such as a protein or a LMM species that degraded quickly and aggregated to migrate as a HMM species or adhered to the column. We caution that the HMM ⁵⁷Fe species observed in some experiments (stimulated by BAC buffer) was not evident in every such experiment. Another possibility is that a cytosolic apo-protein receives Fe from the mitochondrial donor species in a direct transfer such that the donor is never released from the organelle into the supernatant/cytosol.

Our results are most comparable to those of Pandey et al. who found that the mitochondria export a species $(Fe-S)_{int}$ that incorporates into a cytosolic apo-ferredoxin.³¹ Their assay involved incubating mitochondria with buffers that contained the same activation cocktail as we used except with radioactive ³⁵S-cysteine. It also included an apo-ferredoxin that served to receive the exported species. Although they did not directly detect, isolate, or identify (Fe-S)_{int}, they showed that installation of an ISC into the apo-ferredoxin depended on (a) mitochondria that had been incubated with aqueous Fe^{II} and the activation cocktail; (b) mitochondrial proteins involved in ISC assembly (Isu1, Ssq1, and Nfs1), as well as the mitochondrial inner membrane transporter Atm1; and (c) cytosolic proteins involved in the CIA (Dre2 and Cfd1). They directly detected 35S in the native gel band due to ferredoxin. ISCs could be installed into apo-ferredoxin using activated mitochondria in the absence of cytosol. They showed that the solution obtained after removing activated mitochondria, hypothesized to contain (Fe-S)_{int}, was effective in incorporating ISC into cytosolic proteins. However, nearly 4× more ISCs were installed when mitochondria were activated in the presence of cytosol. This boost due to the presence of cytosol led the authors to suggest that mitochondria sense the cytoplasmic demand for ISC biogenesis and then export (Fe-S)_{int} as needed.

Our results are generally consistent and supportive of their results and conclusions. Our results confirm that cytosolic iron-containing proteins require an iron-containing species exported from the mitochondria. Whether that species is low-mass or high-mass or whether it is released free into the cytosol or transferred directly from the mitochondria to a recipient apoprotein remain uncertain. Also uncertain is the identity of the transporter that imports the added aqueous Fe^{II} into mitochondria and the transporter that exports (Fe–S)_{int}/X–S. Another intriguing uncertainty is whether the same pathway is used by mammalian cells where the iron chaperone proteins PCBP1/2, absent in yeast, play a major role in iron trafficking.

CONCLUSIONS

The main conclusions of this study are as follows:

- Some of the aqueous ⁵⁴Fe^{II} that was added to isolated ⁵⁷Fe-enriched mitochondria was imported into the organelle.
- Upon activation with a cocktail that included ATP, GTP, NADH, and cysteine, some of the ⁵⁴Fe that had been loaded into ⁵⁷Fe enriched mitochondria became incorporated into mitochondrial iron-containing proteins.
- When mitochondria were activated, two low-molecular-mass 54Fe- and 57Fe-containing species were exported or released from 54Fe-loaded, 57Fe-enriched intact mitochondria. One of these, called the fast-developing species, was likely an Fe-ATP complex. The other slow-developing species was not assigned, but it could be a complex involving another activation component or a degradation product of an unstable exported species. Whether these iron species were exported from mitochondria via a protein transporter (e.g., Atm1) or released from the mitochondrial surface upon activation remains unestablished.
- When mitochondria were activated, some mitochondrial iron was incorporated into cytosolic proteins. In most experiments, only ⁵⁷Fe-enrichment was observed. Using higher concentrations of cytosol, some ⁵⁴Fe-enrichment was observed.
- Results of this study were interpreted using a "two-pool" working model of mitochondria, in which ⁵⁴Fe is loaded into an "entry" pool that already contains ⁵⁷Fe. The exported or released low-molecular iron species may have come from this pool. The mitochondrial iron installed into cytosolic proteins may have originated from the second "established" pool.

ASSOCIATED CONTENT

Supporting Information

The Supporting Information is available free of charge at https://pubs.acs.org/doi/10.1021/jacs.2c13439.

Materials used; buffers used; iron concentrations of BF buffers and supernatants; iron concentrations of BAC buffers and supernatants; elution volumes for highmolecular mass cytosolic iron-containing species; respirometry traces using isolated mitochondria; concentration of aqueous 54Fe in buffer declined when the mitochondria were resuspended in BF buffer; 54Fe in BF buffer declined when resuspended with the mitochondria when O2 or O2 and CCCP were present; concentration of LMM 54Fe species in SMEs increased after the mitochondria were exposed to BF buffer; LMM iron added to the mitochondria became incorporated into mitochondrial proteins when the mitochondria were activated with AC; iron loaded into the mitochondria became incorporated into mitochondrial proteins upon activation with AC; repeat experiment of Figure S6; LMM iron species were exported from the mitochondria when ISC assembly was stimulated; LMM iron species were exported from AC-activated, 54Fe-loaded, 57Feenriched mitochondria for 120 min at 30 °C; export of LMM Fe was stimulated primarily by *A* and less so by *C*; two LMM iron species were exported from the ACactivated mitochondria regardless of whether the cytosol was included in buffer BAC; ³¹P, ⁵⁴Fe, and ⁵⁶Fe traces of buffers BAC, BACF, and heated BACF; incorporation of 54Fe into cytosolic proteins; little ⁵⁷Fe and ⁵⁴Fe were incorporated into cytosolic proteins when ⁵⁴Fe-loaded and ⁵⁷Fe-enriched mitochondria were incubated in *Bcyt* buffer; mitochondria are required for iron to be incorporated into cytosolic proteins; and ⁵⁴Fe-loaded and ⁵⁷Fe-enriched mitochondria exported modest amounts of ⁵⁷Fe proteins (PDF)

AUTHOR INFORMATION

Corresponding Author

Paul A. Lindahl — Department of Chemistry, Texas A&M University, College Station, Texas 77843-3255, United States; Department of Biochemistry and Biophysics, Texas A&M University, College Station, Texas 77843, United States; Occid.org/0000-0001-8307-9647; Phone: 979-845-0956; Email: Lindahl@chem.tamu.edu; Fax: 979-845-4719

Authors

Rachel E. Shepherd – Department of Chemistry, Texas A&M University, College Station, Texas 77843-3255, United States

Alexia C. Kreinbrink – Department of Biochemistry and Biophysics, Texas A&M University, College Station, Texas 77843, United States

Cybele Lemuh Njimoh – Department of Biochemistry and Biophysics, Texas A&M University, College Station, Texas 77843, United States

Shaik Waseem Vali — Department of Biochemistry and Biophysics, Texas A&M University, College Station, Texas 77843, United States

Complete contact information is available at: https://pubs.acs.org/10.1021/jacs.2c13439

Funding

This work was funded by the National Institutes of Health (GM127021) and the Robert A. Welch Foundation. The content of this article is solely the responsibility of the authors and does not necessarily represent the official views of the NIH or the Welch Foundation.

Notes

The authors declare no competing financial interest.

ACKNOWLEDGMENTS

We thank Debkumar Pain and members of his lab at Rutgers University for providing Leu1 protein. The use of Texas A&M University Microscopy and Imaging Center Core Facility (RRID: SCR 022128) is acknowledged.

ABBREVIATIONS

AA ammonium acetate

ABC ammonium bicarbonate

BPS bathophenanthrolinedisulfonate

FTS flow-through solution

GSH reduced glutathione

GSSG oxidized glutathione

LMM low-molecular-mass

LMP labile metal pool LFeP labile iron pool

LFeP labile from poor

pFTS pseudo flow-through solution

REFERENCES

- (1) Kispal, G.; Csere, P.; Prohl, C.; Lill, R. The Mitochondrial Proteins Atm1p and Nfs1p Are Essential for Biogenesis of Cytosolic Fe/S Proteins. *EMBO* **1999**, *18*, 3981–3989.
- (2) Muhlenhoff, U. The Yeast Frataxin Homolog Yfh1p Plays a Specific Role in the Maturation of Cellular Fe/S Proteins. *Hum. Mol. Genet.* **2002**, *11*, 2025–2036.
- (3) Gerber, J.; Neumann, K.; Prohl, C.; Muhlenhoff, U.; Lill, R. The Yeast Scaffold Proteins Isu1p and Isu2p Are Required inside Mitochondria for Maturation of Cytosolic Fe/S Proteins. *Mol. Cell. Biol.* **2004**, *24*, 4848–4857.
- (4) Froschauer, E. M.; Schweyen, R. J.; Wiesenberger, G. The Yeast Mitochondrial Carrier Proteins Mrs3p/Mrs4p Mediate Iron Transport across the Inner Mitochondrial Membrane. *Biochim. Biophys. Acta, Biomembr.* **2009**, *1788*, 1044–1050.
- (5) Froschauer, E. M.; Rietzschel, N.; Hassler, M. R.; Binder, M.; Schweyen, R. J.; Lill, R.; Mühlenhoff, U.; Wiesenberger, G. The Mitochondrial Carrier Rim2 Co-Imports Pyrimidine Nucleotides and Iron. *Biochem. J.* **2013**, 455, 57–65.
- (6) Knight, S. A. B.; Yoon, H.; Pandey, A. K.; Pain, J.; Pain, D.; Dancis, A. Splitting the Functions of Rim2, a Mitochondrial Iron/Pyrimidine Carrier. *Mitochondrion* **2019**, *47*, 256–265.
- (7) Moore, M. J.; Wofford, J. D.; Dancis, A.; Lindahl, P. A. Recovery of Mrs3Δmrs4Δ *Saccharomyces cerevisiae* Cells under Iron-Sufficient Conditions and the Role of Fe ₅₈₀. *Biochemistry* **2018**, *57*, *672*–*683*.
- (8) McCormick, S. P.; Moore, M. J.; Lindahl, P. A. Detection of Labile Low-Molecular-Mass Transition Metal Complexes in Mitochondria. *Biochemistry* **2015**, *54*, 3442–3453.
- (9) Srour, B.; Gervason, S.; Monfort, B.; D'Autréaux, B. Mechanism of Iron—Sulfur Cluster Assembly: In the Intimacy of Iron and Sulfur Encounter. *Inorganics* **2020**, *8*, 55.
- (10) Sheftel, A. D.; Mason, A. B.; Ponka, P. The Long History of Iron in the Universe and in Health and Disease. *Biochim. Biophys. Acta, Gen. Subj.* **2012**, *1820*, 161–187.
- (11) Berndt, C.; Christ, L.; Rouhier, N.; Mühlenhoff, U. Glutaredoxins with Iron-Sulphur Clusters in Eukaryotes Structure, Function and Impact on Disease. *Biochim. Biophys. Acta Bioenerg.* **2021**, *1862*, 148317.
- (12) Lindahl, P. A.; Vali, S. W. Mössbauer-Based Molecular-Level Decomposition of the Saccharomyces Cerevisiae Ironome, and Preliminary Characterization of Isolated Nuclei. *Metallomics* **2022**, *14*, mfac080.
- (13) Paul, V. D.; Lill, R. SnapShot: Eukaryotic Fe-S Protein Biogenesis. *Cell Metab.* **2014**, *20*, 384–384.e1.
- (14) Lill, R.; Srinivasan, V.; Mühlenhoff, U. The Role of Mitochondria in Cytosolic-Nuclear Iron—Sulfur Protein Biogenesis and in Cellular Iron Regulation. *Curr. Opin. Microbiol.* **2014**, *22*, 111–119.
- (15) Lill, R.; Dutkiewicz, R.; Freibert, S.; Heidenreich, T.; Mascarenhas, J.; Netz, D.; Paul, V.; Pierik, A.; Richter, N.; Stumpfig, M.; Srinivasan, V.; Stehling, O.; Muhlenhoff, U. The role of mitochondria and the CIA machinery in the maturation of cytosolic and nuclear iron—sulfur proteins. *Eur. J. Cell Biol.* **2015**, *94*, 280–291.
- (16) Lange, H.; Lisowsky, T.; Gerber, J.; Mühlenhoff, U.; Kispal, G.; Lill, R. An Essential Function of the Mitochondrial Sulfhydryl Oxidase Erv1p/ALR in the Maturation of Cytosolic Fe/S Proteins. *EMBO Rep.* **2001**, *2*, 715–720.
- (17) Aloria, K.; Schilke, B.; Andrew, A.; Craig, E. A. Iron-Induced Oligomerization of Yeast Frataxin Homologue Yfh1 Is Dispensable in Vivo. *EMBO Rep.* **2004**, *5*, 1096–1101.
- (18) Srinivasan, V.; Pierik, A. J.; Lill, R. Crystal Structures of Nucleotide-Free and Glutathione-Bound Mitochondrial ABC Transporter Atm1. *Science* **2014**, *343*, 1137–1140.
- (19) Lee, J. Y.; Yang, J. G.; Zhitnitsky, D.; Lewinson, O.; Rees, D. C. Structural Basis for Heavy Metal Detoxification by an Atm1-Type ABC Exporter. *Science* **2014**, 343, 1133–1136.
- (20) Fan, C.; Kaiser, J. T.; Rees, D. C. A Structural Framework for Unidirectional Transport by a Bacterial ABC Exporter. *Proc. Natl. Acad. Sci.* **2020**, *117*, 19228–19236.

- (21) Schaedler, T.; Thornton, J.; Kruse, I.; Schwarzlander, M.; Meyer, A.; van Veen, H. W.; Balk, J. A Conserved Mitochondrial ATP-Binding Cassette Transporter Exports Glutathione Polysulfide for Cytosolic Metal Cofactor Assembly*. *J. Biol. Chem.* **2014**, 289, 23264–23274.
- (22) Pandey, A.; Pain, J.; Dziuba, N.; Pandey, A.; Dancis, A.; Lindahl, P.; Pain, D. Mitochondria Export Sulfur Species Required for Cytosolic TRNA Thiolation. *Cell Chem. Biol.* **2018**, 25, 738–748.e3.
- (23) Pain, J.; Balamurali, M. M.; Dancis, A.; Pain, D. Mitochondrial NADH Kinase, Pos5p, Is Required for Efficient Iron-Sulfur Cluster Biogenesis in Saccharomyces cerevisiae*. J. Biol. Chem. 2010, 285, 39409–39424.
- (24) Amutha, B.; Gordon, D. M.; Dancis, A.; Pain, D. Nucleotide-Dependent Iron-Sulfur Cluster Biogenesis of Endogenous and Imported Apoproteins in Isolated Intact Mitochondria. *Mitochondrial Function, Part A: Mitochondrial Electron Transport Complexes and Reactive Oxygen Species; Methods in Enzymology*; Academic Press, 2009; Vol. 456, Chapter 14, pp 247–266.
- (25) Nakai, Y.; Nakai, M.; Lill, R.; Suzuki, T.; Hayashi, H. Thio Modification of Yeast Cytosolic TRNA Is an Iron-Sulfur Protein-Dependent Pathway. *Mol. Cell. Biol.* **2007**, *27*, 2841–2847.
- (26) Qi, W.; Li, J.; Chain, C. Y.; Pasquevich, G. A.; Pasquevich, A. F.; Cowan, J. A. Glutathione Complexed Fe–S Centers. *J. Am. Chem. Soc.* **2012**, *134*, 10745–10748.
- (27) Pearson, S. A.; Wachnowsky, C.; Cowan, J. A. Defining the Mechanism of the Mitochondrial Atm1p [2Fe-2S] Cluster Exporter. *Metallomics* **2020**, *12*, 902–915.
- (28) Li, P.; Hendricks, A. L.; Wang, Y.; Villones, R. L. E.; Lindkvist-Petersson, K.; Meloni, G.; Cowan, J. A.; Wang, K.; Gourdon, P. Structures of Atm1 Provide Insight into [2Fe-2S] Cluster Export from Mitochondria. *Nat. Commun.* **2022**, *13*, 4339.
- (29) Rutherford, J. C.; Ojeda, L.; Balk, J.; Mühlenhoff, U.; Lill, R.; Winge, D. R. Activation of the Iron Regulon by the Yeast Aft1/Aft2 Transcription Factors Depends on Mitochondrial but Not Cytosolic Iron-Sulfur Protein Biogenesis. *J. Biol. Chem.* **2005**, 280, 10135—10140.
- (30) Miao, R.; Kim, H.; Koppolu, U. M. K.; Ellis, E. A.; Scott, R. A.; Lindahl, P. A. Biophysical Characterization of the Iron in Mitochondria from Atm1p-Depleted Saccharomyces cerevisiae. Biochemistry 2009, 48, 9556–9568.
- (31) Pandey, A. K.; Pain, J.; Dancis, A.; Pain, D. Mitochondria Export Iron—Sulfur and Sulfur Intermediates to the Cytoplasm for Iron—Sulfur Cluster Assembly and TRNA Thiolation in Yeast. *J. Biol. Chem.* **2019**, 294, 9489—9502.
- (32) Nguyen, T. Q.; Dziuba, N.; Lindahl, P. A. Isolated *Saccharomyces cerevisiae* Vacuoles Contain Low-Molecular-Mass Transition-Metal Polyphosphate Complexes. *Metallomics* **2019**, *11*, 1298–1309.
- (33) Kim, J. E.; Vali, S. W.; Nguyen, T. Q.; Dancis, A.; Lindahl, P. A. Mössbauer and LC-ICP-MS Investigation of Iron Trafficking between Vacuoles and Mitochondria in Vma2 Δ Saccharomyces cerevisiae. J. Biol. Chem. **2021**, 296, 100141.
- (34) Brawley, H. N.; Lindahl, P. A. Low-Molecular-Mass Labile Metal Pools in *Escherichia coli*: Advances Using Chromatography and Mass Spectrometry. *J. Biol. Inorg. Chem.* **2021**, *26*, 479–494.
- (35) Diekert, K.; de Kroon, I. P. M.; Kispal, G.; Lill, R. Chapter 2 Isolation and Subfractionation of Mitochondria from the Yeast Saccharomyces cerevisiae. Mitochondria; Methods in Cell Biology; Academic Press, 2001; Vol. 65, pp 37–51.
- (36) Djafarzadeh, S.; Jakob, S. M. High-Resolution Respirometry to Assess Mitochondrial Function in Permeabilized and Intact Cells. *J. Vis. Exp.* **2017**, *120*, 54985.
- (37) St-Pierre, J.; Brand, M. D.; Boutilier, R. G. Mitochondria as ATP Consumers: Cellular Treason in Anoxia. *Proc. Natl. Acad. Sci.* **2000**, *97*, 8670–8674.
- (38) Pandey, A.; Pain, J.; Ghosh, A.; Dancis, A.; Pain, D. Fe-S Cluster Biogenesis in Isolated Mammalian Mitochondria Coordinated Use of Persulfide Sulfur and Iron and Requirements for GTP, NADH, and ATP*. J. Biol. Chem. 2015, 290, 640–657.

- (39) Brawley, H. N.; Kreinbrink, A. C.; Hierholzer, J. D.; Vali, S. W.; Lindahl, P. A. The Labile Iron Pool of Isolated *Escherichia coli* Cytosol Likely Includes Fe-ATP and Fe-Citrate but Not Fe-Glutathione or Aqueous Fe. *J. Am. Chem. Soc.* **2023**, *145*, 2104–2117.
- (40) Miao, R.; Martinho, M.; Morales, J. G.; Kim, H.; Ellis, E. A.; Lill, R.; Hendrich, M. P.; Münck, E.; Lindahl, P. A. EPR and Mössbauer Spectroscopy of Intact Mitochondria Isolated from Yah1p-Depleted Saccharomyces cerevisiae. Biochemistry 2008, 47, 9888–9899.
- (41) Garber Morales, J.; Holmes-Hampton, G.; Miao, R.; Guo, Y.; Munck, E.; Lindahl, P. Biophysical Characterization of Iron in Mitochondria Isolated from Respiring and Fermenting Yeast. *Biochemistry* **2010**, *49*, 5436–5444.
- (42) Hudder, B. N.; Morales, J. G.; Stubna, A.; Münck, E.; Hendrich, M. P.; Lindahl, P. A. Electron Paramagnetic Resonance and Mössbauer Spectroscopy of Intact Mitochondria from Respiring Saccharomyces cerevisiae. J. Biol. Inorg. Chem. 2007, 12, 1029–1053.
- (43) Holmes-Hampton, G. P.; Miao, R.; Garber Morales, J.; Guo, Y.; Münck, E.; Lindahl, P. A. A Nonheme High-Spin Ferrous Pool in Mitochondria Isolated from Fermenting *Saccharomyces cerevisiae*. *Biochemistry* **2010**, 49, 4227–4234.
- (44) Zahlten, R. N.; Hochberg, A. A.; Stratman, F. W.; Lardy, H. A. Pyruvate Uptake in Rat Liver Mitochondria: Transport or Adsorption? *FEBS Lett.* **1972**, *21*, 11–13.
- (45) Goucher, C. R.; Taylor, J. F. Compounds of Ferric Iron with Adenosine Triphosphate and Other Nucleoside Phosphates. *J. Biol. Chem.* **1964**, 239, 2251–2255.